Published in final edited form as:
J Neurosci. 2009 July 15; 29(28): 9090–9103. doi:10.1523/JNEUROSCI.1357-09.2009.

Impaired Balance of Mitochondria Fission and Fusion in Alzheimer Disease

Xinglong Wang[1], **Bo Su**[1], **Hyoung-gon Lee**[1], **Xinyi Li**[1], **George Perry**[1,2], **Mark A. Smith**[1], and **Xiongwei Zhu**[1]

[1]Department of Pathology, Case Western Reserve University, Cleveland, Ohio USA

[2]College of Sciences, University of Texas at San Antonio, San Antonio, Texas USA

Abstract

Mitochondrial dysfunction is a prominent feature of Alzheimer disease (AD) neurons. In this study, we explored the involvement of an abnormal mitochondrial dynamics by investigating the changes in the expression of mitochondrial fission and fusion proteins in AD brain and the potential cause and consequence of these changes in neuronal cells. We found that mitochondria were redistributed away from axons in the pyramidal neurons of AD brain. Immunoblot analysis revealed that levels of DLP1 (also referred to as Drp1), OPA1, Mfn1, and Mfn2 were significantly reduced while levels of Fis1 were significantly increased in AD. Despite their differential effects on mitochondrial morphology, manipulations of these mitochondrial fission and fusion proteins in neuronal cells to mimic their expressional changes in AD, caused a similar abnormal mitochondrial distribution pattern, such that mitochondrial density was reduced in the cell periphery of M17 cells or neuronal process of primary neurons and correlated with reduced spine density in the neurite. Interestingly, oligomeric amyloid-β-derived diffusible ligands (ADDLs) caused mitochondrial fragmentation and reduced mitochondrial density in neuronal processes. More importantly, ADDL-induced synaptic change (i.e., loss of dendritic spine and PSD-95 puncta) correlated with abnormal mitochondrial distribution. DLP1 overexpression, likely through repopulation of neuronal processes with mitochondria, prevented ADDLs-induced synaptic loss, suggesting that abnormal mitochondrial dynamics plays an important role in ADDLs-induced synaptic abnormalities. Based on these findings, we suggest that an altered balance in mitochondrial fission and fusion is likely an important mechanism leading to mitochondrial and neuronal dysfunction in AD brain.

Keywords

amyloid-β-derived diffusible ligands; Alzheimer disease; DLP1/Drp1; mitochondrial dynamics; synaptic abnormality; Hippocampus

INTRODUCTION

Characterized by neurofibrillary tangles, senile plaques, and progressive loss of neuronal cells in selective brain regions, Alzheimer disease (AD) is a fatal degenerative dementia with initial memory impairment that progresses to a total debilitating loss of mental and physical faculties (Smith, 1998). Evidence suggests that memory failure in AD is a result of synaptic loss and, among all the early changes that occur in AD, is a robust correlate of AD-associated cognitive deficits, leading to the notion that synaptic dysfunction plays a critical role in the pathogenesis

Corresponding Author: Xiongwei Zhu, Ph.D. Department of Pathology Case Western Reserve University 2103 Cornell Road Cleveland, Ohio 44106 USA Tel: 216-368-5903 Fax: 216-368-8964 xiongwei.zhu@case.edu.

of AD (DeKosky and Scheff, 1990; Terry et al., 1991; Coleman et al., 2004). A myriad of studies have focused on the central role of amyloid-β (Aβ) in the pathogenesis and progression of AD. Aβ oligomers may bind to dendritic spines, causing synaptic dysfunction (Lacor et al., 2004), however, the molecular mechanism remains elusive.

In mammals, mitochondria are vital organelles known for their essential role in energy metabolism and cell survival (Delettre et al., 2000; Benard et al., 2007). Neurons are particularly vulnerable to mitochondrial dysfunction because of their high metabolic rate dependence and complex morphology (Delettre et al., 2000; Benard et al., 2007). More specifically, mitochondria are of pivotal importance for synaptic development and plasticity, and changes in mitochondria distribution and/or function can result in synaptic dysfunction and loss (Li et al., 2004; Verstreken et al., 2005). Notably, while defects in mitochondrial function are a prominent early event in AD (Blass et al., 2000; Swerdlow and Kish, 2002; Zhu et al., 2004; Bubber et al., 2005), whether and how mitochondrial defects contribute to synaptic dysfunction in AD neurons is unclear.

Emerging evidence suggests that mitochondria are dynamic organelles undergoing constant fission and fusion regulated by a machinery involving large dynamin-related GTPases (Chan, 2006). Mitochondrial dynamics not only determines mitochondrial morphology and size, but also regulates mitochondrial distribution and function (Chan, 2006). Given the critical role of mitochondria in neurons, impaired mitochondrial dynamics is increasingly implicated in neurodegenerative diseases including Parkinson and Huntington diseases (Exner et al., 2007; Deng et al., 2008; Mortiboys et al., 2008; Poole et al., 2008; Yang et al., 2008; Park et al., 2009; Wang et al., 2009). In relation to AD, Aβ caused rapid and severe impairment of mitochondrial transport (Rui et al., 2006). More recently, we demonstrated an abnormal mitochondrial morphology and distribution in AD fibroblasts compared to normal healthy fibroblasts from age-matched controls (Wang et al., 2008a) and found that amyloid-β protein precursor (AβPP) overexpression, through Aβ overproduction, caused abnormal mitochondrial dynamics in neurons (Wang et al., 2008b). In this study, we aimed to determine whether an imbalance in mitochondrial fission and fusion occurs *in vivo* in AD neurons by exploring the expression of mitochondrial fission/fusion proteins [i.e., DLP1 (also referred to as Drp1), Fis1, OPA1 and Mfn1/2] in AD brain and identifying the potential cause and consequence of changes in these proteins related to mitochondrial dynamics and synaptic function.

MATERIALS AND METHODS

Cell culture and transfection

The human neuroblastoma cell lines, M17 were grown in Opti-MEM® I medium (Invitrogen), supplemented with 5% or 10% (v/v) fetal bovine serum and 1% penicillin-streptomycin, in 5% CO_2 in a humid incubator at 37°C. Cells were transfected using Effectene (QIAGEN) according to the manufacturer's instructions. For co-transfection, a 3:1 ratio (indicated plasmid: mito-DsRed2) was applied. Regular culture medium containing 300 μg/ml geneticin (Invitrogen), 20 μg/ml Blasticidin (Invitrogen), or 150 μg/ml of hygromycin B (Calbiochem) was used for stable cell line selection. The selective medium was replaced every 3 days until the appearance of foci, each apparently derive from a single stably transfected cell. Stable cell lines were then picked and maintained with 100 μg/ml geneticin, 5 μg/ml Blasticidin, or 30 μg/ml of hygromycin. Primary neurons from E18 rat hippocampus (BrainBits) were seeded at 30,000-40,000 cells per well on 8-well chamber slides coated with Poly-D-Lysine/Laminin (BD) in neurobasal medium supplemented with 2% B27 (Invitrogen)/0.5 mM glutamine/25 mM glutamate. Half the culture medium was changed every 3 days with neurobasal medium supplemented with 2% B27 (Invitrogen) and 0.5 mM glutamine. All cultures were kept at 37° C in a humidified 5% CO_2 containing atmosphere. More than 90% of the cells were neurons after they were cultured for 7-17 days of culture *in vitro* (DIV), which was verified by positive

staining for the neuronal specific markers microtubule-associated protein-2 (MAP2, dendritic marker) and Tau-1 (axonal marker). At DIV7-12, neurons were transfected using Neurofect (Genlantis) according to manufacturer's protocol.

Expression vectors and antibodies

Mito-DsRed2 construct (Clontech), GFP tagged wild type DLP1, mutant DLP1 K38A and Fis1 constructs (gifts from Dr. Yisang Yoon, University of Rochester), YFP tagged PSD-95 (gift from Dr. Ann Marie Craig, University of British Columbia, Canada), and wild type OPA1 and mutant OPA1 K301A constructs (gifts from Dr. Luca Scorrano, Venetian Institute of Molecular Medicine, Italy) were obtained. The expression plasmids for myc tagged wild type DLP1/DLP1 K38A were constructed based on the pCMV-Tag3 Vector (Stratagene), while myc/GFP tagged wild type OPA1/OPA1 K301A was based on pCMV-Tag Vector (Stratagene) and pcDNA3.1 (Invitrogen) respectively. The miR RNAi vector was generated via the pcDNA 6.2-GW/ EmGFP-miR construct (Invitrogen). The miR RNAi sequence targeting the open reading frame region of human or rat mitochondria fission or fusion proteins are: human OPA1 (ATCACTTGCAAGATAAGCTGG), rat OPA1(GCGCAGTATTGTTACAGACTT), human Mfn2(CTCCTTAGCAGACACAAAGAA), rat Mfn2(GCTGGACAGCTGGATTGATAA), human Mfn1(ATTTCTTCCCATACCATCCTC), rat Mfn1 (GCAAACAAGGTTTCTTGTGCA), human Fis1(TTACGGATGTCATCATTGTAC), and rat Fis1(TGGTGCCTGGTTCGAAGCAA A). miR RNAi construct targeting both human and rat DLP1 was described as previously (Wang et al., 2008a). Primary antibodies used included mouse anti-DLP1/OPA1 (BD), mouse anti-Mfn1 (Novus Biologicals), mouse anti-Mfn2/COX I (Sigma), rabbit anti-Fis1 (Imgenex), mouse anti-GAPDH (Chemicon), rabbit anti-α-tubulin (Epitomics), rabbit anti-phospho-DLP1 (Ser616) (Cell signaling) and mouse anti-α-tubulin/ Myc/COX IV (Cell Signaling)..

Immunocytochemical procedures

Hippocampal, frontal cortical and cerebellar brain tissue obtained postmortem was fixed and 6 μm-thick consecutive sections prepared essentially as described previously (Zhu et al., 2000). Cases used in this study included AD (n = 5) and control cases (n = 5). Immunocytochemistry was performed by the peroxidase anti-peroxidase protocol as described before (Zhu et al., 2000). Absorption experiments were performed to verify the specificity of antibody binding. Each case was examined on a Zeiss Axiophot-microscope for neurons stained with DLP1, OPA1, Mfn1, Mfn2, Fis1, COXI (Molecular Probes), and Tubulin. Positively-stained neurons were counted.

Western blot analysis

Brain samples from gray matter of temporal cortex of AD (n = 13, ages = 60-89 years, postmortem interval = 1-24 h) and age-matched control (n = 12, ages = 58-92 years; postmortem interval = 2-23 h) cases based on clinical and pathological criteria established by CERAD and an NIA consensus panel (Khachaturian and Emr, 1984; Mirra, 2000) or cells, were lysed with 1×Cell Lysis Buffer (Cell Signaling), plus 1 mM PMSF (Sigma) and Protease Inhibitor Cocktail (Sigma). Equal amounts of total protein extract (5 μg or 20 μg) were resolved by SDS-PAGE and transferred to Immobilon-P (Millipore). Following blocking with 10% nonfat dry milk, primary and secondary antibodies were applied as previously described (Wang et al., 2008a) and the blots developed with Immobilon Western Chemiluminescent HRP Substrate (Millipore).

Electron microscopy

Hippocampus tissue fixed in 2% parafromaldehyde was embedded in LR Gold after ethanol dehydration and polymerized with UV exposure. Sections (60-100 nm) were placed on nickel

grids and incubated with COX antibody followed by gold-conjugated secondary antibody. Grids were stained with uranyl acetate and lead citrate and viewed in a Zeiss electron microscope at 80 kV (CEM902; Zeiss, Oberkochen, Germany).

Cell treatments and measurements

ADDLs was prepared using $A\beta_{1\text{-}42}$ peptide (California Peptide, Napa, CA, USA) as described before (Klein, 2002), except that phenol red free neurobasal medium (Invitrogen, USA) was used instead of phenol red free F12 medium. Primary hippocampal cells were usually treated at DIV7-16. The negative control $A\beta_{42\text{-}1}$ peptide (Anaspec) was subject to the same preparation procedure as ADDLs. Cytotoxicity was measured by Cytotoxicity Detection Kit (LDH; Roche). For differentiation of M17 cells, serum content was reduced to 2% and 1 μM retinoic acid (Sigma-Aldrich) was included in the culture media.

To measure mitochondrial ROS, the fluorescent probe MitoSOX (Invitrogen) was used according to manufacturer's protocol. Briefly, neurons were incubated with 2.5 μM MitoSOX in culture media for 10 min, followed by three times wash with pre-warmed Hanks' balanced salt solution (Invitrogen). Cells were fixed in 37% paraformaldehyde 4% for 30 min, and then stained and observed using a Zeiss LSM 510 inverted fluorescence microscope.

Mitochondria were harvested from human brain samples or cells using a mitochondrial isolation kit (Pierce) following the manufacturer's protocol. The cytosolic extracts were also used to determine DLP1 levels. The biotin-switch assay was performed using an S-Nitrosylated Protein Detection Assay Kit (Cayman) following the manufacturer's protocol. Biotinylated DLP1 was immunoprecipitated with anti-DLP1 antibody in RIPA buffer using Protein G-agarose beads (Roche Diagnostics) according to manufacturer's protocol, and analyzed by western blot using Avidin-HRP (Cayman).

Immunofluorescence

Cells were cultured on chamber slides. After treatment, cells were fixed and stained as described previously (Wang et al., 2008a). All fluorescence images were captured with a Zeiss LSM 510 inverted fluorescence microscope or a Zeiss LSM 510 inverted laser-scanning confocal fluorescence microscope. Confocal images of far red fluorescence were collected using 633-nm excitation light from a HeNe laser and a 650-nm long pass filter; Images of mito-DsRed2 red fluorescence were collected using 543-nm excitation light from an argon laser and a 560-nm long pass filter; and, green fluorescence images were collected using 488-nm excitation light from an argon laser and a 500-550-nm band pass barrier filter. Image analysis was performed with open-source image-analysis programs WCIF ImageJ (developed by W. Rasband).

Time-lapse imaging

Neurons were seeded in glass-bottomed dishes (MatTek) and then transfected with Mito-Dendra2. 48 h after transfection, cells were placed in a well-equipped live imaging station (Zeiss CTI-Controller 3700) with controlled CO_2 content, humidity and temperature of stage, objective and the air. Images were captured with a Zeiss LSM 510 inverted laser-scanning confocal fluorescence microscope. Images of red signal were collected using 543-nm excitation light from an argon laser and a 560-nm long pass filter; And, Green fluorescence were collected using 488-nm excitation light from an argon laser and a 500-550-nm band pass barrier filter. During time-lapse imaging, frames were captured every 10s for at least 1h without apparent phototoxicity or photobleaching. Image analysis was also performed with open-source image-analysis programs WCIF ImageJ (developed by W. Rasband).

RESULTS

Changes in levels and distribution of mitochondrial fission/fusion proteins in neurons from AD hippocampus

We investigated the expression pattern of mitochondrial fission (i.e., DLP1 and Fis1) and fusion proteins (i.e., OPA1, Mfn1, and Mfn2) in hippocampal tissues from 13 AD patients and 12 age-matched normal subjects. Immunoblot analysis revealed significant changes in the levels of all five proteins: DLP1 levels were dramatically reduced by 74.3% in AD brains; OPA1, Mfn1 and Mfn2 levels were also reduced by 61.4%, 27.8% and 33.6%, respectively. Interestingly, unlike other fission/fusion proteins, Fis1 levels were significantly increased 4.8 fold in AD brains compared to age-matched control brains (Figure 1A,B). No significant changes in overall mitochondrial contents were noted between AD and control samples as evidenced by the constant expression levels of COX-IV, a mitochondrial marker (Figure 1A). Real-time PCR studies of 5 control and 5 AD cases confirmed a 60% increase in Fis1 mRNA levels in AD but no changes in mRNA levels of other mitochondrial fission/fusion proteins (not shown). Immunocytochemical analysis of these proteins revealed extensive immunoreactivity of each of these proteins in pyramidal neurons in hippocampal tissues from age-matched control patients (Figure 1C). Interestingly, only background neuronal immunoreactivity of DLP1 was noted in the hippocampus from AD patients (Figure 1C), consistent with the greatly reduced levels revealed by immunoblot analysis. In contrast, extensive neuronal immunoreactivity was noted for the other four mitochondrial fission/fusion proteins in hippocampal tissues from AD patients, however, they displayed a distinctive distribution pattern compared to that of control hippocampus (Figure 1C). Although all these proteins demonstrate a uniform distribution throughout the soma and neurites of pyramidal neurons in age-matched control hippocampus, in AD hippocampal neurons, they accumulated in the soma and were depleted in the neurite (Figure 1C). Positively-stained neurons were counted and categorized into three groups: neurons with only soma staining, neurons with only axon staining or neurons with both axon and soma staining. Indeed, all these four proteins (i.e., Fis1, OPA1, Mfn1, and Mfn2) demonstrated only soma staining in more than 80% of pyramidal neurons in AD hippocampus, significantly different from that of control hippocampal neurons (Figure 1D). Antibodies against each of these fission/fusion proteins from two different sources were used in both immunocytochemical and immunoblot studies and similar results were obtained (not shown). The specificity of each antibody was confirmed by pre-absorption of primary antibodies with their immunizing peptides. Since Fis1, Mfn1, and Mfn2 are mitochondrial outer membrane proteins and OPA1 is a mitochondrial inner membrane protein, the consistent pattern of their re-distribution to soma in AD pyramidal neurons implies that mitochondria are re-distributed in these neurons.

Mitochondria are redistributed in AD pyramidal neurons

To confirm the altered distribution of mitochondria in AD neurons, we employed a widely used mitochondrial marker, cytochrome c oxidase subunit 1 (COX-1), which also demonstrated exclusive neuronal staining in both AD and age-matched control cases (Figure 2A). The mitochondrial localization of COX-1 in pyramidal neurons was confirmed by electron microscopy (Figure 2B). Notably, immunocytochemical analysis also revealed striking changes in the distribution of COX-1 immunoreactivity within neurons between AD and control cases: localization of COX-1 in control cases is seen throughout the soma and processes of most pyramidal neurons (>85%) of the hippocampus, while in AD cases, the immunoreactivity is essentially limited to the soma with no more than 20% neurons demonstrating positively stained processes. Since some neurons may lose processes in sections due to the angle of cutting in both AD and control cases which may mask the difference, to further clarify the changes in COX-1 distribution, immunofluorescence analysis of tubulin and COX-1 double staining of AD and age-matched control hippocampal tissues was performed

(Figure 2C). Quantitative analysis of tubulin staining revealed no significant difference in the percentage of neurons with soma staining only, neurite staining only or both soma and processes staining between AD and age-matched control sections (Figure 2D). However, in control cases, the majority (>90%) of those neurons with long processes contains COX-1 throughout the soma and processes while in AD cases, only a minority of those neurons with long processes contain COX-1 in the soma and processes (<20%) and the majority of those neurons with long processes contains COX-1 only in the soma (Figure 2C and D). Since COX-1 is a mitochondrial inner membrane protein widely used as a mitochondrial marker, this finding confirms that mitochondria accumulate in the soma and are reduced in neuronal processes in AD pyramidal neurons.

Changes in sub-cellular localization and modification of DLP1 in AD brain

Previously we reported shorter mitochondria in AD neurons (Wang et al., 2008b), suggestive of enhanced mitochondrial fission. DLP1 is known to play a critical role in the fission process, however, our results indicated reduced levels of DLP1 in AD neurons. Given that the majority of DLP1 in mammalian cells is cytosolic and it is the mitochondrial DLP1 that participates in mitochondrial fission (Smirnova et al., 2001), we hypothesized that there may be comparable or even increased levels of mitochondrial DLP1 in AD compared to control brain samples. To test this hypothesis, we conducted subcellular fractionation experiments from AD and control brain homogenates and the resultant fractions were analyzed by probing immunoblots with anti-DLP1 antibody as well as antibodies for GAPDH to track cytosolic fractions, and COX-IV to track mitochondrial fractions. We found slightly increased levels of mitochondrial DLP1 (not significant) in AD brain samples (Figure 3A). The immunoblot analysis also confirmed significantly reduced levels of cytosolic DLP1 in AD samples (Figure 3A). Phosphorylation of DLP1 at several sites regulates its mitochondrial fission activity: while there is still debate over whether phosphorylation of DLP1 at Ser637 enhances or inhibits mitochondrial fission activity (Cereghetti et al., 2008; Han et al., 2008), it appears that phosphorylation of DLP1 at Ser 616 activates mitochondrial fission activity (Taguchi et al., 2007). Given the known imbalance of kinase and phosphatase activities such that increased phosphorylation of multiple proteins were identified in AD brain, we determined the levels of DLP1 phosphorylated at Ser616 in AD brain and found significantly increased phosphorylated DLP1 at this site in both mitochondrial and cytosolic fractions from AD brains compared to control brains (Figure 3A). A recent study suggested that S-nitrosylation of DLP1 activates GTPase activity and mitochondrial fission and reported increased S-nitrosylation of DLP1 in AD brain tissues (Cho et al., 2009), we also determined DLP1 nitrosylation in our studies by biotin-switch assay. Indeed, we confirmed significantly increased S-nitrosylation of DLP1 in AD brain tissues (Figure 3B). These data suggest that, despite the reduction in overall levels of DLP1, there were comparable levels of mitochondrial DLP1 in AD neurons which likely contribute to enhanced mitochondrial fission.

Modulations of mitochondrial fission/fusion proteins, mimicking changes in AD neurons, cause abnormal mitochondrial distribution in M17 cells

Since mitochondrial fission/fusion proteins not only control mitochondrial morphology, but also regulate mitochondrial distribution, we hypothesized that changes in mitochondrial fission/fusion proteins may also change mitochondrial morphology and distribution in AD neurons. To test this hypothesis, we evaluated whether changes in these proteins, mimicking the changes found in AD neurons, affected mitochondrial morphology and distribution in M17 human neuroblastoma cell line. Stable M17 cell lines were generated with reduced expression of DLP1, OPA1, Mfn1, and Mfn2, i.e., mitochondrial fission/fusion proteins that demonstrated reduced levels in AD neurons, and overexpression of Fis1, i.e., the mitochondrial fission/fusion protein that demonstrated increased levels in AD neurons. The overexpression or reduced expression of mitochondrial fission/fusion proteins was confirmed by western blotting (Figure

4A). There was no increase in basal cell death in any of the cell lines compared to control cells (i.e., untransfected or empty vector-transfected cells) (data not shown). To visualize mitochondria, stable M17 cell lines were transiently transfected with Mito-DsRed 2. 48 h after transfection, cells were fixed, stained and evaluated using laser confocal microscopy (Figure 4B). Detailed analysis of mitochondrial length revealed that these manipulations, mimicking changes in AD neurons, caused differential effects on mitochondrial morphology: The majority of the M17 cells in control lines demonstrated short tubular form mitochondria; Almost 100% cells in M17 stable cells with reduced DLP1 expression demonstrated elongated mitochondria while the majority of M17 cells with reduced OPA1, Mfn1 or Mfn2 expression or increased Fis1 expression demonstrated fragmented mitochondria (72.6 ± 8.1%, 77.4 ± 7.3%, 63.2 ± 4.2%, and 84.7 ± 6.4%, respectively) (Figure 4C). Most notably, despite their differential effects on morphology, all manipulations caused a similar abnormal effect on mitochondrial distribution when compared to untransfected or empty vector-transfected control cells: In control cells, mitochondria were distributed evenly throughout the cytoplasm (>95% cells, Figure 4D). However, in M17 stable cells with reduced DLP1 expression, almost 100% of the cells demonstrated an abnormal mitochondrial distribution with mitochondria aggregating in the perinuclear area while more remote cytoplasmic areas were devoid of mitochondria; 63.5 ± 3.2%, 87.8 ± 3.2%, 78.3 ± 5.3%, and 82.5 ± 7.3% of cells in the M17 stable cell lines with reduced OPA1, Mfn1, or Mfn2 expression or increased Fis1 expression, respectively, demonstrated a similar abnormal mitochondrial distribution (Figure 4D).

We also generated stable M17 cell lines overexpressing dominant negative DLP1 or OPA1 mutants. As expected, they caused effects similar to DLP1 or OPA1 knockdown on mitochondrial morphology and distribution (Figure 4C,D): overexpression of the DLP1 K38A mutant caused elongated mitochondria while overexpression of OPA1 K301A mutant caused fragmented mitochondria (Figure 4C), but both caused abnormal mitochondrial distribution with mitochondria accumulating in the perinuclear area (Figure 4D).

In addition, we further generated stable M17 cells lines overexpressing DLP1 or OPA1 or with reduced expression of Fis1, i.e., changes opposite to that observed in AD neurons (Figure 4C,D). The analysis of mitochondrial morphology and distribution in these cell lines revealed that DLP1 overexpression caused primarily fragmented mitochondria, and Fis1 knockdown caused primarily elongated mitochondria, while overexpression of OPA1 in cells resulted in a heterogeneous population of mitochondria that vary in shape (Figure 4C). However, neither of these manipulations caused abnormal perinuclear accumulation of mitochondria (Figure 4D).

Modulations of mitochondrial fission/fusion proteins, mimicking changes in AD, cause abnormal mitochondrial distribution in differentiated primary neuronal cells

To study the effect of modulating this mitochondrial fission/fusion expression in differentiated cells, primary rat hippocampal neurons (DIV 7-12) were transfected with GFP-tagged miR RNAi expression vectors targeting DLP1, OPA1, Mfn1, or Mfn2 or a myc-tagged Fis1 expression vector. Cells were fixed and stained 3 or 4 days after transfection. Positively transfected cells can be identified by GFP fluorescence or Myc immunostaining. In non-transfected control hippocampal neurons, mitochondria were abundant and overlapping in soma and proximal neurites, but were separated from each other and evenly distributed in distal neurites and usually demonstrated short tubular forms with an average length of 2.1 ± 0.08 μm (Figure 5A,B). In DLP1 knockdown neurons, many mitochondria in neurites became extremely long (>10μm) and the average mitochondrial length increased significantly (4.1 ± 0.56 μm) (Figure 5B). However, mitochondrial number was significantly reduced in neuronal processes (Figure 5C), leaving large lengths of neurites devoid of mitochondria (Figure 5E). Indeed, the neurite mitochondrial index (total mitochondrial length/neurite length) in neuronal

processes 200 μm in length beginning from the cell body as an index for mitochondrial coverage in neuronal processes was significantly decreased (Figure 5D). OPA1, Mfn1, and Mfn2 knockdown as well as Fis1 overexpression caused mitochondria to become globular and significantly shorter in positively-transfected neurons (Figure 5A,B). Mitochondrial aggregates were often observed in the neuronal processes of Mfn1 knockdown or Fis1 overexpressing neurons. Most importantly, despite their differential effect on mitochondrial morphology compared to DLP1 knockdown, manipulations of OPA1, Mfn1, Mfn2, or Fis1 all caused significantly reduced neuritic mitochondrial density (Figure 5C), decreased neurite mitochondrial index (Figure 5D) and increased length of neurites devoid of mitochondria in the neuronal processes (Figure 5E) in positively-transfected hippocampal neurons, a phenomenon also observed in DLP1 knockdown neurons, consistent with the re-distribution pattern of mitochondria in M17 cells.

Differentiated hippocampal neurons were also transiently transfected with dominant negative DLP1 or OPA1 mutants and essentially caused effects similar to DLP1 or OPA1 knockdown on mitochondrial morphology and distribution (Figure 5B-E). In contrast, overexpression of DLP1 caused fragmented mitochondria but increased mitochondrial number in neuronal processes with an overall increase in neurite mitochondrial index (Figure 5B-E). OPA1 overexpression led to a heterogeneous effect on mitochondrial morphology and Fis1 knockdown caused mitochondria elongation, but neither changed mitochondrial density in neuronal processes or neurite mitochondrial index in rat primary neurons (Figure 5B-E).

Effect of mitochondria fission/fusion proteins on dendritic spines

As one approach to determine whether alterations in mitochondrial dynamics correlate with neuronal changes, we compared the number of dendritic spines, an important index of synaptic plasticity. Rat E18 primary hippocampal neurons (DIV9) were transfected with GFP-tagged miR RNAi expression vectors targeting DLP1, OPA1, Mfn1, or Mfn2 or a myc-tagged Fis1 expression vector together with mito-DsRed2 to label mitochondria. Three days later, neurons were fixed and stained. Positively transfected neurons were identified by GFP fluorescence or Myc immunostaining. For each neuron, dendritic segments with 100-200 μm in length beginning 100 μm from the cell body were selected. In dendrites with large diameter, mitochondria were overlapping and abundant in the proximal area, but separated from each other in the distal area similar to those in dendrites with small diameter. Protrusions of 0.5-5 μm in length that had a clear neck and expanded mushroom-like heads or a stubby shape were defined as dendritic spines. At DIV 12, dendrites of control neurons were extensively covered with dendritic spines (Figure 6A). However, neurons with DLP1 downregulation showed a markedly reduced spine density (1.1 ± 0.35/10 μm) compared to non-transfected or control RNAi-transfected neurons (4.2 ± 0.46/10 μm). Similarly OPA1, Mfn1, or Mfn2 knockdown as well as Fis1 overexpression also caused markedly reduced spine density (Figure 6A and B). To determine whether these changes correlated with a loss of mitochondria in the vicinity of the spine, the frequency of spine occupancy by mitochondria was measured. It was found that the number of spines containing at least one mitochondrion in a 1 μm diameter region centered in the middle of the spine was significantly reduced in all neurons with DLP1/OPA1/Mfn1/Mfn2 knockdown or Fis1 overexpression (Figure 6C).

Effects of Aβ on mitochondrial dynamics in primary neurons

It is believed that soluble Aβ oligomers are involved in the pathogenesis of AD. We previously demonstrated that AβPP overexpression, likely through Aβ overproduction, induce mitochondrial dysfunction through altered mitochondrial dynamics (Wang et al., 2008b). It was reported that $A\beta_{25\text{-}35}$ induced mitochondrial fragmentation prior to cell death. To directly examine the potential effect of Aβ oligomers on mitochondria, rat hippocampal neurons (DIV: 7-9) were co-transfected with a GFP expression vector to label cell shape and mito-DsRed2 to

highlight mitochondria, respectively. Two days after transfection, neurons were incubated with 800 nM oligomeric amyloid-β-derived diffusible ligands (ADDLs). As a control, in parallel experiments, neurons were treated with 10 μM $A\beta_{42-1}$, the reverse peptide was subjected to the same preparation steps as ADDLs. After treatment for 24 h, cells were fixed, stained and imaged by laser confocal microscopy. Treatment with ADDLs led to significantly reduced mitochondrial length in neurites, suggestive of enhanced mitochondrial fragmentation (Figure 7A,B). More importantly, unlike the vehicle- or $A\beta_{42-1}$-treated controls, large segments of neurites were devoid of mitochondria (Figure 7E). In fact, the neuritic mitochondrial density and the neurite mitochondrial index were also significantly reduced in neuronal processes of ADDLs-treated primary neurons (Figure 7C,D). The negative control, $A\beta_{42-1}$ had no effect on any of these mitochondrial parameters.

The readily discernible individual mitochondrion in distal neurites makes it possible to measure the occurrence of mitochondrial fusion and fission events. A fusion event was defined as two separate mitochondria moving towards each other, forming a physical connection into one intact organelle and moving together. A fission event was recognized by the division of a single mitochondrion into two distinct mitochondria. Both fission and fusion events were counted in the segment of axon around 100 μm in length beginning 300 μm from the cell body of control or ADDLs-treated neurons during 20 min time-lapse recordings. Mitochondria rapidly underwent constant fission and fusion in control neurons (0.0263 ± 0.0102 events/μm in 20 min for fusion and 0.0399 ± 0.0098 events/μm in 20 min for fusion) (Figure 7F,G). Similar rates were seen in neurons treated with the reverse peptide $A\beta_{42-1}$. In contrast, mitochondria fission and fusion occurred at a much slower frequency in neurons treated with ADDLs (0.0036 ± 0.0019 events/μm in 20 min for fusion and 0.0048 ± 0.002 events/μm in 20 min for fusion), suggesting that both mitochondrial fission and fusion were impaired in ADDLs-treated primary neurons (Figure 7F,G). Further, the ratio of the total time each mitochondrion involved in fission/fusion spent in the post-fission, “single state” (defined as the time interval from fission to fusion) and post-fusion, “fused state” (defined as the time interval from fusion to fission) during the 20 min recording time were determined. In both control neurons and those treated with $A\beta_{42-1}$, the total time of each mitochondrion spent in the post-fusion state and post-fission state was similar (Figure 7H). However, in the ADDLs-treated neurons, mitochondria spent significantly less time in the post-fusion state compared to post-fission state (Figure 7H).

We next sought to determine whether Aβ oligomers induced changes in the expression of these mitochondrial fission and fusion proteins in rat hippocampal neurons. Primary neurons (DIV: 7~12) were incubated with different doses of ADDLs (50 nM-10 μM) for 24 h or with 800 nM ADDLs for various period of time (0-24 h) and cell lysates were prepared for immunoblot analysis of mitochondrial fission and fusion proteins. As a negative control, neurons were also treated with 10 μM $A\beta_{42-1}$ for 24 h. No apparent cell death under these conditions with either ADDLs or $A\beta_{42-1}$ treatments was observed as determined by LDH assay (data not shown). Interestingly, ADDLs treatment caused a significantly decrease in DLP1 and OPA1 levels in a dose-dependent manner (Figure 7I,J), while there was no significant change in Mfn1, Mfn2, or Fis1 level (data not shown). In fact, 800 nM ADDLs treatment induced a significant reduction in DLP1 or OPA1 levels as early as 2 h and the effect lasted for at least 24 h (Figure 7K and L). In contrast, $A\beta_{42-1}$ treatment did not change mitochondria fission and fusion protein levels compared with untreated or vehicle-treated neurons (Figure 7M).

We further determined the levels of DLP1 in the mitochondrial fraction and found that Aβ oligomers induced significantly increased levels of mitochondrial DLP1 (Figure 8A). Similar to AD brain, increased mitochondrial DLP1 was accompanied by Aβ oligomers-induced increased levels of phosphorylation (Figure 8A) and S-nitrosylation of DLP1 (Figure 8B).

Effects of DLP1 and OPA1 on Aβ-induced alterations in mitochondrial dynamics

To determine the role of DLP1 and/or OPA1 in Aβ-induced abnormal mitochondrial morphology and distribution, rat hippocampal neurons (DIV 9) were transiently transfected with Myc-tagged wild type DLP1 (DLP1wt) or GFP-tagged OPA1 (OPA1wt). Mito-DsRed2 was cotransfected to label mitochondria. Two days after transfection, neurons were treated with 800 nM ADDLs for 24 h, fixed and stained. Positively transfected cells were selected based on DsRed fluorescence signal and Myc immunoreactivity (or GFP fluorescence signal). As shown before, in the absence of ADDLs treatment, mitochondria became fragmented in neurons overexpressing DLP1, but were more heterogeneous in shape with an increase in average mitochondrial length in neurons overexpressing OPA1 (Figure 9C). Mitochondrial number and coverage in the neuronal processes were increased in neurons overexpressing DLP1 but unchanged in neurons overexpressing OPA1 (Figure 9A,B). In control primary neurons expressing only vector, ADDLs induced mitochondrial fragmentation, reduced mitochondrial number and neuritic mitochondrial index as well as increased average length of neuritic segments devoid of mitochondria in the neuronal processes (Figure 9B-E). Interestingly, in the presence of ADDLs, OPA1 overexpression restored mitochondrial length comparable to untreated controls (Figure 9C). However, OPA1 overexpression had no effects on ADDLs-induced decrease in mitochondria number and neurite mitochondrial index or increase in average length of neuritic segments devoid of mitochondria in the neuronal processes in positively-transfected primary neurons (Figure 9A-E). On the other hand, in contrast to OPA1-overexpressing neurons, in the presence of ADDLs, DLP1 overexpression did not change mitochondrial length but restored mitochondrial number, neurite mitochondrial index and average length of neuritic segments devoid of mitochondria to a level comparable to untreated controls in positively-transfected neurons (Figure 9A-E).

Effects of DLP1 and OPA1 on Aβ-induced functional changes

Mitochondria serve as the primary source of endogenous reactive oxygen species (ROS). By using a fluorescence red dye MitoSOX to measure mitochondrial ROS production, we were able to demonstrate that treatment of rat hippocampal neurons with ADDLs resulted in a large increase of mitochondria ROS levels in rat hippocampal neurons (Figure 10A, B). In the absence of ADDLs treatment, OPA1 overexpression led to significantly decreased basal level of mitochondrial ROS as evidenced by the lower fluorescent signal in positively-transfected cells compared to those neighboring non-transfected cells and GFP vector-transfected control cells (Figure 10A, B). However, DLP1 overexpression did not significantly change the basal mitochondrial ROS levels. Similarly, in the presence of ADDLs treatment, OPA1 overexpression significantly lowered mitochondrial ROS levels to that comparable to untreated controls, while DLP1 overexpression had no effects (Figure 10A, B).

Consistent with previous findings demonstrating that ADDLs treatment negatively impacted synaptic function (Lacor et al., 2004), we found that 24 h treatment with 800 nM ADDLs also induced a significantly reduced dendritic spine number in rat hippocampal neurons (DIV12) (Figure 10C, D). Notably, in the presence of ADDLs treatment, DLP1 overexpression significantly alleviated ADDLs-induced decreases in dendritic spine number (Figure 10C, D). In contrast, OPA1 overexpression had no effects on dendritic spine number with or without ADDLs treatment. We further studied the effects of ADDLs treatment on excitatory synapses by measuring the expression of postsynaptic density protein 95 (PSD-95) in primary neurons (Figure 10E, F). We transfected primary neurons (DIV9) with YFP tagged PSD-95 to label excitatory synapses and mito-DsRed2 to label mitochondria together with or without Myc-tagged wild type DLP1 or OPA1 (OPA1wt). At DIV 11, neurons were treated with 800 nM ADDLs for 24 h and then fixed. Positively transfected cells were selected based on YFP/DsRed fluorescence signal and Myc immunoreactivity. In the absence of ADDLs treatment, DLP1 overexpression led to increased number of PSD-95 puncta while OPA1 overexpression had no

effect on puncta number (Figure 10E, F). As expected, ADDLs treatment significantly decreased the number of PSD-95 puncta (Figure 10E, F). Interestingly, ADDLs-induced reduction in PSD-95 puncta number was effectively prevented by DLP1 overexpression but not by OPA1 overexpression. Overall, these data suggested that DLP1-regulated mitochondria distribution played an important role in ADDLs-induced change of dendritic spines and synapses plasticity.

DISCUSSION

In this study, we demonstrated significant alterations in the expression pattern of mitochondrial fission/fusion proteins in hippocampal tissues from AD compared to age-matched control brain. We found reduced levels of DLP1/OPA1/Mfn1/Mfn2 and increased levels of Fis1 in AD hippocampus, consistent with the notion that mitochondrial dynamics are altered in AD. More importantly, all of these proteins accumulated in the soma and were depleted in neuronal processes in AD neurons. Given that OPA1, Mfn1/2, and Fis1 are mitochondrial membrane proteins, these data suggest a potential redistribution of mitochondria in AD neurons. In this regard, we also demonstrated that COX-I, a widely used mitochondrial marker, was redistributed in a similar pattern, confirming that mitochondria are redistributed in AD neurons. To explore the consequence of changes in the expression levels of mitochondrial fission/fusion proteins, the expression of these proteins was manipulated in M17 cells and primary hippocampal neurons in a way that mimicked their expression changes in AD. Although these manipulations caused different effects on mitochondrial morphology, they all caused reduced mitochondrial density in the cell periphery (M17 cells) or neuronal processes (primary neurons) which correlated with reduced spine numbers (primary neurons), suggesting that the altered expression of these proteins may play an important role in mitochondrial re-distribution and synaptic dysfunction in AD neurons. In an attempt to address the potential cause of abnormal mitochondrial dynamics, we found that ADDL-treatment not only led to mitochondrial fragmentation, consistent with prior studies (Barsoum et al., 2006), but also led to mitochondrial depletion from neuronal processes. ADDLs likely caused abnormal mitochondrial dynamics directly through adverse effects on DLP1 and OPA1 expression since DLP1 overexpression rescued ADDL-induced abnormal mitochondrial distribution while OPA1 overexpression restored ADDL-induced mitochondrial fragmentation. Most importantly, we found that ADDL-induced mitochondrial depletion from dendrites correlated with reduced dendritic spine density and PSD-95 puncta number, which could be effectively reversed by DLP1 overexpression through repopulation of neuronal processes with mitochondria, suggesting that abnormal mitochondrial dynamics plays an important role in ADDL-induced synaptic dysfunction and loss.

Our prior finding of reduced mitochondrial length in the soma of AD neurons compared to controls suggested that an abnormal mitochondrial dynamics towards enhanced fission may be involved in neuronal dysfunction in AD (Wang et al., 2008b). The major finding of the current study is an altered expression pattern of mitochondrial fission and fusion proteins *in vivo* in AD brain, confirming that the balance of mitochondrial fission and fusion is indeed tipped in AD neurons, which thus likely contributes to mitochondrial dysfunction and neurodegeneration *in vivo*. However, although OPA1/Mfn1/Mfn2 reduction or Fis1 overexpression could lead to mitochondrial fragmentation, DLP1 reduction could cause mitochondrial elongation and thus may make the net effect on mitochondrial morphology uncertain (Chan, 2006). Interestingly, despite the overall reduction in DLP1 levels, we found mitochondrial DLP1 levels remained similar between AD and control samples and are increased in ADDL-treated neurons. In this regard, it is of interest to note that DLP1 phosphorylation at Ser616 and S-nitrosylation activate its mitochondrial fission activity (Taguchi et al., 2007; Cho et al., 2009) and we found increased DLP1 phosphorylation and S-nitrosylation in AD and ADDL-treated neurons. Given that the majority of DLP1 in mammalian

cells is cytosolic and it is the mitochondrial DLP1 that participates in mitochondrial fission (Smirnova et al., 2001), the comparable or increased mitochondrial DLP1 levels in AD or ADDL-treated samples, coupled with increased DLP1 S-nitrosylation, suggested that changes in DLP1 in AD and ADDL-treated neurons, along with changes in other fission/fusion proteins, likely contributes to enhanced mitochondrial fission. Such a notion is obviously supported by the net outcome of mitochondrial fragmentation in ADDL-treated neurons.

Interestingly, a detailed measurement of mitochondrial fission and fusion events in ADDL-treated primary neurons revealed that although neuronal mitochondria are still capable of fusing and dividing, they fuse and divide at a significantly slower rate, suggesting that both fission and fusion are impaired, consistent with altered expression of both fission and fusion proteins. It is unclear whether a slower but still balanced mitochondria fission and fusion process has any effect on mitochondrial function. Notably, although both fission and fusion slowed down at a similar rate, we found that mitochondria switched from spending a similar time in the post-fusion, “fused state” and post-fission, “single state” in control cells to spending the majority of their time in the post-fission, “single state” in ADDL-treated cells, which is likely the reason that a net outcome of decreased mitochondrial length was observed in these cells. Such a switch of steadystate morphology is likely due to the reduced expression of OPA1 caused by ADDLs treatment because recent studies demonstrated that non-fusing mitochondria are characterized by reduced OPA1 expression and that OPA1 depletion in individual mitochondrion may preclude its fusion even if surrounded by fusion-competent mitochondria (Twig et al., 2008).

Our results also showed that the distribution of mitochondrial membrane proteins OPA1/Mfn1/Mfn2/Fis1 was altered in AD neurons such that neuronal processes were devoid of these proteins, a mitochondrial re-distribution in AD neurons that was also confirmed with a more widely used mitochondrial marker, COX-1. Intracellular mitochondria distribution is of critical importance to neurons since the great morphological complexity and dependency on mitochondria for energy at multiple selective sites make neurons particularly sensitive to perturbations in mitochondrial distribution (Kann and Kovacs, 2007). The loss of mitochondria from axon terminals leads to synaptic dysfunction in flies (Stowers et al., 2002; Melov, 2004; Guo et al., 2005). Most interestingly, in relation to mitochondrial distribution, we demonstrated in M17 neuroblastoma cells that, knockdown of DLP1/OPA1/Mfn1/Mfn2 or overexpression of Fis1, conditions that mimic changes in AD neurons, all caused perinuclear accumulation of mitochondria, leaving more remote areas of the cell devoid of mitochondria. Similarly, all of these manipulations also resulted in a significant reduction of mitochondrial density and uneven mitochondrial coverage in neuronal processes in differentiated primary hippocampal neurons with significantly greater axial neurite length devoid of mitochondria. Our data suggest that changes in the expression of these mitochondrial fission and fusion proteins likely underlie abnormal mitochondrial distribution in AD neurons.

Many in the field believe that Aβ plays a central role in the pathogenesis of AD (Kamenetz et al., 2003). Early changes in the AD brain include loss of synapses and synaptic loss is the most robust correlate of AD-associated cognitive deficits. Aβ is a homeostatic regulator of synaptic strength (Kamenetz et al., 2003) suggesting that perturbations in soluble Aβ levels might be linked to the learning and memory deficits in AD patients (Masliah et al., 2001). Indeed, AD mouse models with elevated Aβ levels exhibit decreased neuronal synaptophysin and PSD-95 staining as well as dendritic spine loss (Mucke et al., 2000; Lanz et al., 2003; Almeida et al., 2005; Spires et al., 2005) along with learning deficits well before the formation of senile plaques. Application of Aβ or soluble oligomers (e.g., ADDLs), either *in vitro* or *in vivo*, adversely affects LTP and synaptic transmission (Lambert et al., 1998; Walsh et al., 2002; Wang et al., 2002; Cleary et al., 2005). Along this line, Aβ overexpression decreases spine density (Hsieh et al., 2006) and ADDLs directly bind to dendritic spines (Lacor et al., 2004) and induce abnormalities in spine composition, shape and abundance (Lacor et al., 2007).

However, it remains unclear how these Aβ effects are transduced to synaptic dysfunction. In this study, we found that ADDLs induced mitochondrial fragmentation accompanied by a decrease in mitochondria coverage in neurites. At the same time, ADDL-treatment also caused significant decreases in the levels of both DLP1 and OPA1. Functionally, ADDLs treatment increased mitochondrial ROS levels and decreased spine density and PSD 95-positive puncta. It was reported that number of dendritic mitochondria affected the number and plasticity of spines and synapses and, indeed, there is a correlation between dendritic spine morphogenesis and recruitment of nearby mitochondria (Li et al., 2004). In our study, we found that DLP1 overexpression could not prevent mitochondria ROS overproduction induced by ADDLs, but could efficiently alleviate synaptic loss or dysfunction caused by ADDLs, suggesting that mitochondrial distribution regulated by DLP1 probably accounted for the synaptic dysfunction induced by ADDLs. On the other hand, we showed that OPA1 could alleviate ADDLs-induced ROS overproduction by mitochondria. These data suggest that OPA1 plays an important role in ADDLs-induced mitochondria dysfunction and yet one cannot rule out the possibility that OPA1 is also involved in ADDLs-induced synaptic abnormalities through its effect on mitochondria function.

Taken together, our data demonstrate significant changes in the expression and distribution of mitochondrial fission and fusion proteins *in vivo* in AD and suggest altered mitochondrial dynamics likely contribute to mitochondrial and neuronal dysfunction in disease pathogenesis. We further found that Aβ-induced abnormal mitochondrial dynamics plays an important role in Aβ-induced mitochondrial dysfunction and synaptic dysfunction. Modulating the expression of mitochondrial fission and fusion proteins likely represents a potential novel therapeutic strategy for treating AD.

Acknowledgments

This study is supported by the NIH (AG031852) and Alzheimer's Association (IIRG-07-60196).

REFERENCES

Almeida CG, Tampellini D, Takahashi RH, Greengard P, Lin MT, Snyder EM, Gouras GK. Beta-amyloid accumulation in APP mutant neurons reduces PSD-95 and GluR1 in synapses. Neurobiology of disease 2005;20:187–198. [PubMed: 16242627]

Barsoum MJ, Yuan H, Gerencser AA, Liot G, Kushnareva Y, Graber S, Kovacs I, Lee WD, Waggoner J, Cui J, White AD, Bossy B, Martinou JC, Youle RJ, Lipton SA, Ellisman MH, Perkins GA, Bossy-Wetzel E. Nitric oxide-induced mitochondrial fission is regulated by dynamin-related GTPases in neurons. The EMBO journal 2006;25:3900–3911. [PubMed: 16874299]

Benard G, Bellance N, James D, Parrone P, Fernandez H, Letellier T, Rossignol R. Mitochondrial bioenergetics and structural network organization. Journal of cell science 2007;120:838–848. [PubMed: 17298981]

Blass JP, Sheu RK, Gibson GE. Inherent abnormalities in energy metabolism in Alzheimer disease. Interaction with cerebrovascular compromise. Annals of the New York Academy of Sciences 2000;903:204–221. [PubMed: 10818509]

Bubber P, Haroutunian V, Fisch G, Blass JP, Gibson GE. Mitochondrial abnormalities in Alzheimer brain: mechanistic implications. Ann Neurol 2005;57:695–703. [PubMed: 15852400]

Cereghetti GM, Stangherlin A, Martins de Brito O, Chang CR, Blackstone C, Bernardi P, Scorrano L. Dephosphorylation by calcineurin regulates translocation of Drp1 to mitochondria. Proc Natl Acad Sci U S A 2008;105:15803–15808. [PubMed: 18838687]

Chan DC. Mitochondrial fusion and fission in mammals. Annual review of cell and developmental biology 2006;22:79–99.

Cho DH, Nakamura T, Fang J, Cieplak P, Godzik A, Gu Z, Lipton SA. S-nitrosylation of Drp1 mediates beta-amyloid-related mitochondrial fission and neuronal injury. Science 2009;324:102–105. [PubMed: 19342591]

Cleary JP, Walsh DM, Hofmeister JJ, Shankar GM, Kuskowski MA, Selkoe DJ, Ashe KH. Natural oligomers of the amyloid-beta protein specifically disrupt cognitive function. Nature neuroscience 2005;8:79–84.

Coleman P, Federoff H, Kurlan R. A focus on the synapse for neuroprotection in Alzheimer disease and other dementias. Neurology 2004;63:1155–1162. [PubMed: 15477531]

DeKosky ST, Scheff SW. Synapse loss in frontal cortex biopsies in Alzheimer's disease: correlation with cognitive severity. Annals of neurology 1990;27:457–464. [PubMed: 2360787]

Delettre C, Lenaers G, Griffoin JM, Gigarel N, Lorenzo C, Belenguer P, Pelloquin L, Grosgeorge J, Turc-Carel C, Perret E, Astarie-Dequeker C, Lasquellec L, Arnaud B, Ducommun B, Kaplan J, Hamel CP. Nuclear gene OPA1, encoding a mitochondrial dynamin-related protein, is mutated in dominant optic atrophy. Nat Genet 2000;26:207–210. [PubMed: 11017079]

Deng H, Dodson MW, Huang H, Guo M. The Parkinson's disease genes pink1 and parkin promote mitochondrial fission and/or inhibit fusion in Drosophila. Proc Natl Acad Sci U S A 2008;105:14503–14508. [PubMed: 18799731]

Exner N, Treske B, Paquet D, Holmstrom K, Schiesling C, Gispert S, Carballo-Carbajal I, Berg D, Hoepken HH, Gasser T, Kruger R, Winklhofer KF, Vogel F, Reichert AS, Auburger G, Kahle PJ, Schmid B, Haass C. Loss-of-function of human PINK1 results in mitochondrial pathology and can be rescued by parkin. J Neurosci 2007;27:12413–12418. [PubMed: 17989306]

Guo XF, Macleod GT, Wellington A, Hu F, Panchumarthi S, Schoenfield M, Marin L, Charlton MP, Atwood HL, Zinsmaier KE. The GTPase dMiro is required for axonal transport of mitochondria to Drosophila synapses. Neuron 2005;47:379–393. [PubMed: 16055062]

Han XJ, Lu YF, Li SA, Kaitsuka T, Sato Y, Tomizawa K, Nairn AC, Takei K, Matsui H, Matsushita M. CaM kinase I alpha-induced phosphorylation of Drp1 regulates mitochondrial morphology. J Cell Biol 2008;182:573–585. [PubMed: 18695047]

Hsieh H, Boehm J, Sato C, Iwatsubo T, Tomita T, Sisodia S, Malinow R. AMPAR removal underlies Abeta-induced synaptic depression and dendritic spine loss. Neuron 2006;52:831–843. [PubMed: 17145504]

Kamenetz F, Tomita T, Hsieh H, Seabrook G, Borchelt D, Iwatsubo T, Sisodia S, Malinow R. APP processing and synaptic function. Neuron 2003;37:925–937. [PubMed: 12670422]

Kann O, Kovacs R. Mitochondria and neuronal activity. American journal of physiology 2007;292:C641–657. [PubMed: 17092996]

Khachaturian ZS, Emr M. Research Workshop on the Diagnosis of Alzheimer-Disease. Neurobiology of aging 1984;5:161–162.

Klein WL. A beta toxicity in Alzheimer's disease: globular oligomers (ADDLs) as new vaccine and drug targets. Neurochemistry International 2002;41:345–352. [PubMed: 12176077]

Lacor PN, Buniel MC, Furlow PW, Clemente AS, Velasco PT, Wood M, Viola KL, Klein WL. Abeta oligomer-induced aberrations in synapse composition, shape, and density provide a molecular basis for loss of connectivity in Alzheimer's disease. J Neurosci 2007;27:796–807. [PubMed: 17251419]

Lacor PN, Buniel MC, Chang L, Fernandez SJ, Gong Y, Viola KL, Lambert MP, Velasco PT, Bigio EH, Finch CE, Krafft GA, Klein WL. Synaptic targeting by Alzheimer's-related amyloid beta oligomers. J Neurosci 2004;24:10191–10200. [PubMed: 15537891]

Lambert MP, Barlow AK, Chromy BA, Edwards C, Freed R, Liosatos M, Morgan TE, Rozovsky I, Trommer B, Viola KL, Wals P, Zhang C, Finch CE, Krafft GA, Klein WL. Diffusible, nonfibrillar ligands derived from Abeta1-42 are potent central nervous system neurotoxins. Proceedings of the National Academy of Sciences of the United States of America 1998;95:6448–6453. [PubMed: 9600986]

Lanz TA, Carter DB, Merchant KM. Dendritic spine loss in the hippocampus of young PDAPP and Tg2576 mice and its prevention by the ApoE2 genotype. Neurobiology of disease 2003;13:246–253. [PubMed: 12901839]

Li Z, Okamoto K, Hayashi Y, Sheng M. The importance of dendritic mitochondria in the morphogenesis and plasticity of spines and synapses. Cell 2004;119:873–887. [PubMed: 15607982]

Masliah E, Mallory M, Alford M, DeTeresa R, Hansen LA, McKeel DW Jr. Morris JC. Altered expression of synaptic proteins occurs early during progression of Alzheimer's disease. Neurology 2001;56:127–129. [PubMed: 11148253]

Melov S. Modeling mitochondrial function in aging neurons. Trends in Neurosciences 2004;27:601–606. [PubMed: 15374671]

Mirra S. Vascular lesions and the consortium to establish a registry for Alzheimer's disease (CERAD). Brain Pathology 2000;10:591–591.

Mortiboys H, Thomas KJ, Koopman WJ, Klaffke S, Abou-Sleiman P, Olpin S, Wood NW, Willems PH, Smeitink JA, Cookson MR, Bandmann O. Mitochondrial function and morphology are impaired in parkin-mutant fibroblasts. Ann Neurol 2008;64:555–565. [PubMed: 19067348]

Mucke L, Masliah E, Yu GQ, Mallory M, Rockenstein EM, Tatsuno G, Hu K, Kholodenko D, Johnson-Wood K, McConlogue L. High-level neuronal expression of abeta 1-42 in wild-type human amyloid protein precursor transgenic mice: synaptotoxicity without plaque formation. J Neurosci 2000;20:4050–4058. [PubMed: 10818140]

Park J, Lee G, Chung J. The PINK1-Parkin pathway is involved in the regulation of mitochondrial remodeling process. Biochem Biophys Res Commun 2009;378:518–523. [PubMed: 19056353]

Poole AC, Thomas RE, Andrews LA, McBride HM, Whitworth AJ, Pallanck LJ. The PINK1/Parkin pathway regulates mitochondrial morphology. Proceedings of the National Academy of Sciences of the United States of America 2008;105:1638–1643. [PubMed: 18230723]

Rui Y, Tiwari P, Xie Z, Zheng JQ. Acute impairment of mitochondrial trafficking by beta-amyloid peptides in hippocampal neurons. J Neurosci 2006;26:10480–10487. [PubMed: 17035532]

Smirnova E, Griparic L, Shurland DL, van der Bliek AM. Dynamin-related protein Drp1 is required for mitochondrial division in mammalian cells. Mol Biol Cell 2001;12:2245–2256. [PubMed: 11514614]

Smith MA. Alzheimer disease. International review of neurobiology 1998;42:1–54. [PubMed: 9476170]

Spires TL, Meyer-Luehmann M, Stern EA, McLean PJ, Skoch J, Nguyen PT, Bacskai BJ, Hyman BT. Dendritic spine abnormalities in amyloid precursor protein transgenic mice demonstrated by gene transfer and intravital multiphoton microscopy. J Neurosci 2005;25:7278–7287. [PubMed: 16079410]

Stowers RS, Megeath LJ, Gorska-Andrzejak J, Meinertzhagen IA, Schwarz TL. Axonal transport of mitochondria to synapses depends on milton, a novel Drosophila protein. Neuron 2002;36:1063–1077. [PubMed: 12495622]

Swerdlow RH, Kish SJ. Mitochondria in Alzheimer's disease. International review of neurobiology 2002;53:341–385. [PubMed: 12512346]

Taguchi N, Ishihara N, Jofuku A, Oka T, Mihara K. Mitotic phosphorylation of dynamin-related GTPase Drp1 participates in mitochondrial fission. The Journal of biological chemistry 2007;282:11521–11529. [PubMed: 17301055]

Terry RD, Masliah E, Salmon DP, Butters N, DeTeresa R, Hill R, Hansen LA, Katzman R. Physical basis of cognitive alterations in Alzheimer's disease: synapse loss is the major correlate of cognitive impairment. Annals of neurology 1991;30:572–580. [PubMed: 1789684]

Twig G, Elorza A, Molina AJ, Mohamed H, Wikstrom JD, Walzer G, Stiles L, Haigh SE, Katz S, Las G, Alroy J, Wu M, Py BF, Yuan J, Deeney JT, Corkey BE, Shirihai OS. Fission and selective fusion govern mitochondrial segregation and elimination by autophagy. EMBO J 2008;27:433–446. [PubMed: 18200046]

Verstreken P, Ly CV, Venken KJ, Koh TW, Zhou Y, Bellen HJ. Synaptic mitochondria are critical for mobilization of reserve pool vesicles at Drosophila neuromuscular junctions. Neuron 2005;47:365–378. [PubMed: 16055061]

Walsh DM, Klyubin I, Fadeeva JV, Cullen WK, Anwyl R, Wolfe MS, Rowan MJ, Selkoe DJ. Naturally secreted oligomers of amyloid beta protein potently inhibit hippocampal long-term potentiation in vivo. Nature 2002;416:535–539. [PubMed: 11932745]

Wang H, Lim PJ, Karbowski M, Monteiro MJ. Effects of overexpression of huntingtin proteins on mitochondrial integrity. Hum Mol Genet 2009;18:737–752. [PubMed: 19039036]

Wang HW, Pasternak JF, Kuo H, Ristic H, Lambert MP, Chromy B, Viola KL, Klein WL, Stine WB, Krafft GA, Trommer BL. Soluble oligomers of beta amyloid (1-42) inhibit long-term potentiation but not long-term depression in rat dentate gyrus. Brain Res 2002;924:133–140. [PubMed: 11750898]

Wang X, Su B, Fujioka H, Zhu X. Dynamin-like protein 1 reduction underlies mitochondrial morphology and distribution abnormalities in fibroblasts from sporadic Alzheimer's disease patients. The American journal of pathology 2008a;173:470–482. [PubMed: 18599615]

Wang X, Su B, Siedlak SL, Moreira PI, Fujioka H, Wang Y, Casadesus G, Zhu X. Amyloid-beta overproduction causes abnormal mitochondrial dynamics via differential modulation of mitochondrial fission/fusion proteins. Proceedings of the National Academy of Sciences of the United States of America 2008b;105:19318–19323. [PubMed: 19050078]

Yang Y, Ouyang Y, Yang L, Beal MF, McQuibban A, Vogel H, Lu B. Pink1 regulates mitochondrial dynamics through interaction with the fission/fusion machinery. Proc Natl Acad Sci U S A 2008;105:7070–7075. [PubMed: 18443288]

Zhu X, Smith MA, Perry G, Aliev G. Mitochondrial failures in Alzheimer's disease. American journal of Alzheimer's disease and other dementias 2004;19:345–352.

Zhu XW, Rottkamp CA, Boux H, Takeda A, Perry G, Smith MA. Activation of p38 kinase links tau phosphorylation, oxidative stress, and cell cycle-related events in Alzheimer disease. Journal of neuropathology and experimental neurology 2000;59:880–888. [PubMed: 11079778]

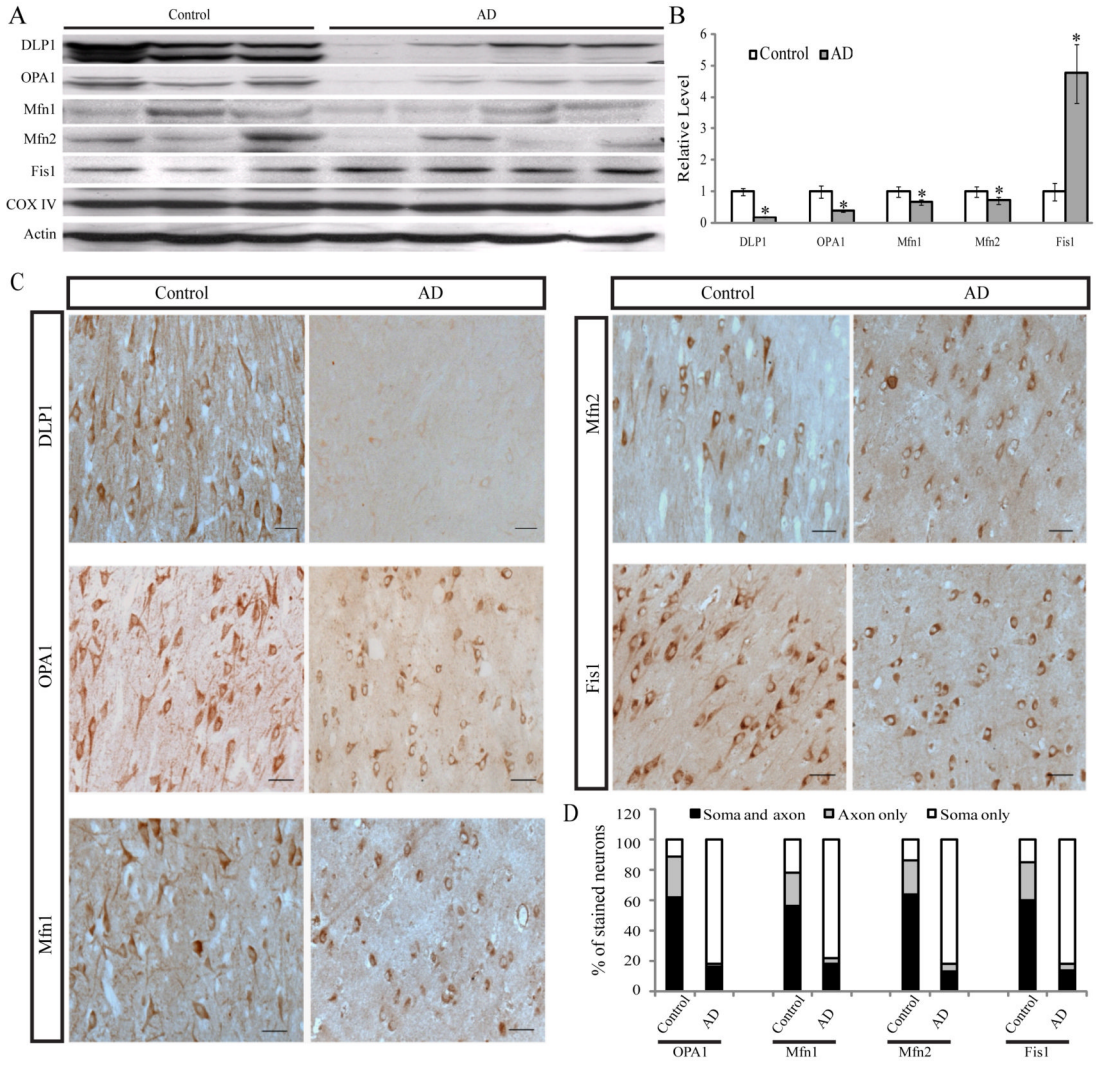

Figure 1.

Mitochondria fission and fusion protein expression and distribution in AD hippocampus. Representative immunoblot (A) and quantification analysis (B) revealed that in AD hippocampus (n=13), levels of DLP1/OPA1/Mfn1/Mfn2 were reduced significantly, while levels of Fis1 were increased significantly compared with age-matched controls (n=12) (*$p < 0.05$, student t-test). Equal protein amounts (30 μg) were loaded and confirmed with actin staining (A). (C): Representative immunocytochemistry of DLP1, OPA1, Mfn1, Mfn2, and Fis1 in hippocampus from AD (right panel) and age-matched controls (left panel). All scale bars: 50 μm. (D) Positively-stained neurons were categorized int`o three groups: neurons with only soma staining, neurons with only axon staining or neurons with both axon and soma staining. Quantification in 5 AD brains and 5 age-matched controls indicated that Fis1, OPA1, Mfn1, and Mfn2 demonstrated soma staining in more than 80% of pyramidal neurons in AD hippocampus, significantly different from that of control hippocampal neurons (D).

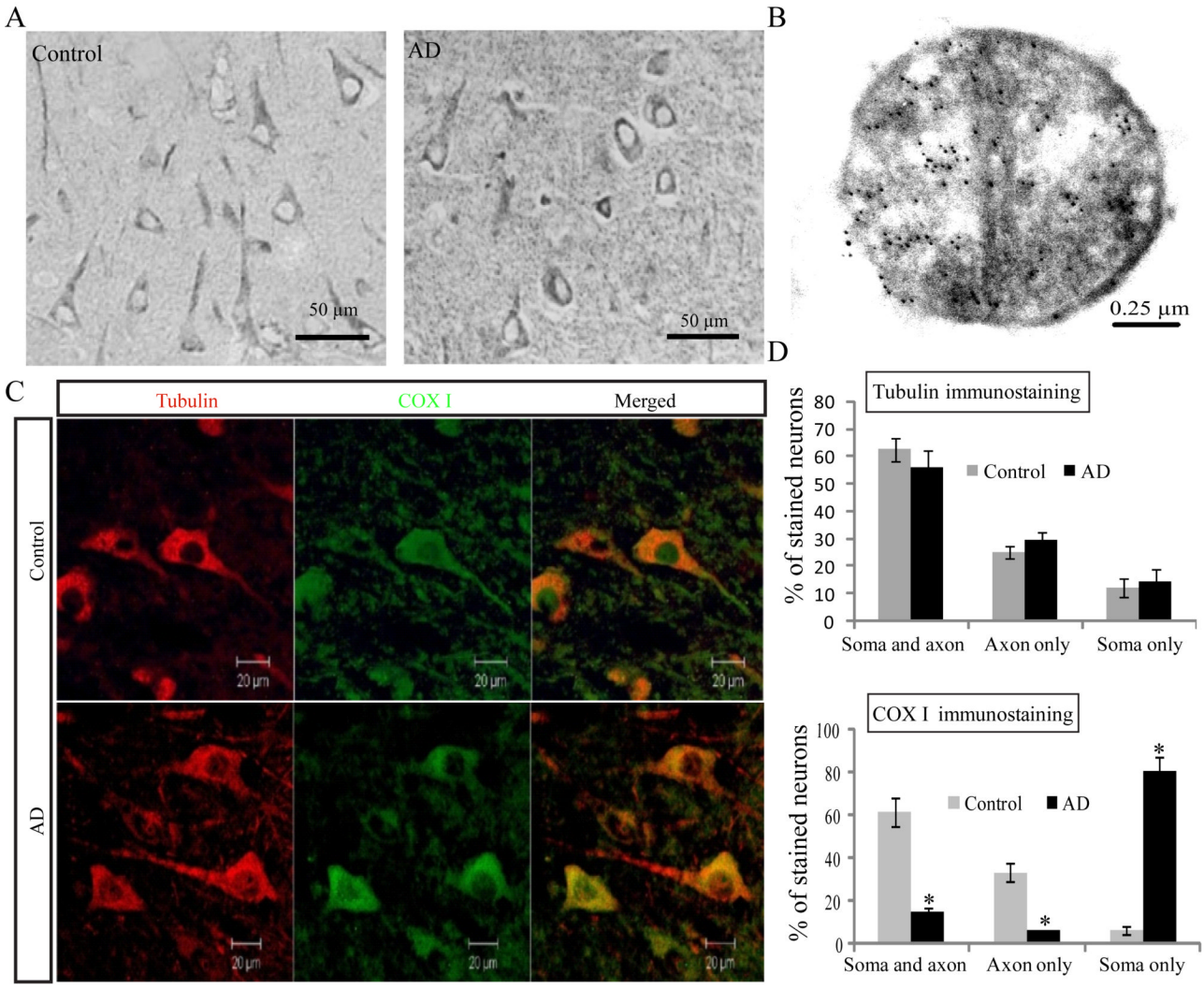

Figure 2.

Altered distribution of mitochondria in AD. Representative immunocytochemistry of COX I (A) confirmed that, in AD hippocampus, COX I staining of neuronal processes was significantly reduced compared with age-matched controls (*$p < 0.05$, student t-test). (B) A representative immunoelectron micrograph of COX I gold labeling of mitochondria is shown. (C) A representative immunofluorescence picture of COX I staining (green) and tubulin (red) in AD hippocampus (lower panel) and age-matched control (upper panel). Quantification (D) revealed that mitochondria were evenly distributed in the control (n=5), while they were significantly constricted in the soma in AD hippocampus (n=5) (*$p < 0.05$, student t-test).

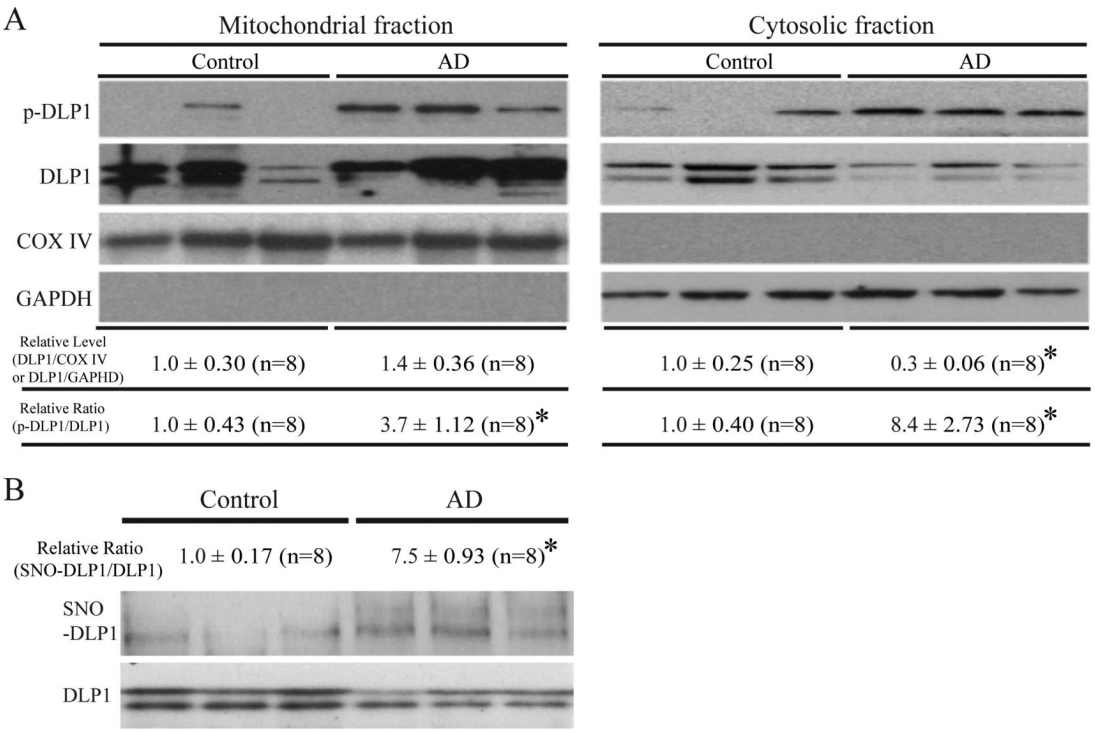

Figure 3.

Changes in sub-cellular localization and modification of DLP1 in AD brain. Representative immunoblot and quantification analysis (A) of DLP1 and phospho-DLP1 (Ser616) (p-DLP1) in the mitochondrial and cytosolic fraction from AD brains (n=8) and age-matched controls brains (n=8) indicated that, although relative mitochondrial DLP1 level (DLP1/COX IV) did not change significantly, the relative ratio of p-DLP1/DLP1 increased significantly in both mitochondrial and cytosolic fraction from AD brain samples (A). All samples were also immunoblotted with antibodies to detect mitochondrial (COX IV) and cytoplasmic (GAPDH) markers. The absence of GAPDH in the mitochondrial fraction confirms the purity of preparations from brain tissues. Representative immunoblot and quantification analysis (B) of S-nitrosylated DLP1 (SNO-DLP1) by biotin-switch assay of AD brains (n=8) and age-matched controls brains (n=8) showed that relative SNO-DLP1 formation increased significantly in AD. All experiments were repeated three times (*$p < 0.05$, student-t-test).

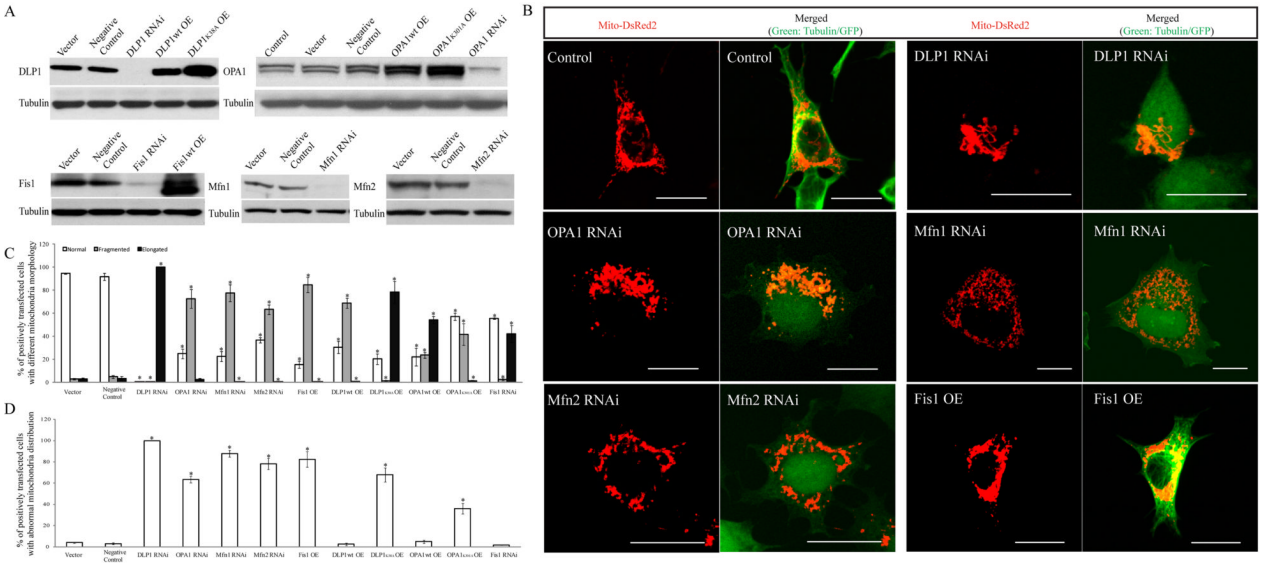

Figure 4.

Modulations of mitochondrial fission/fusion proteins, mimicking changes in AD neurons, cause abnormal mitochondrial distribution in M17 cells. (A) Representative immunoblot analysis of M17 cells stably knocking down or overexpressing mitochondrial fission and fusion proteins. Equal protein amounts (15 μg) were loaded. Tubulin immunoblot was used as an internal loading control. (B) showed representative confocal pictures of mitochondria in M17 cells either stably overexpressing (OE) or knocking down (RNAi) mitochondria fission/fusion proteins. Cells were transfected with Mito-DsRed2 to label mitochondria. For knockdown experiments, GFP was tagged to the miRNAi construct. For overexpression experiments, tubulin was immunostained as green to label the cell shape. Quantifications of mitochondria morphology (C) and distribution (D) in M17 cell either stably overexpressing or knocking down mitochondria fission/fusion proteins revealed differential effects on mitochondrial morphology but similar abnormal effect on mitochondrial distribution for those manipulations mimicking changes in AD. All scale bars: 20 μm. At least 500 cells were analyzed in triplicate for each cell line (*$p < 0.05$, student-t-test).

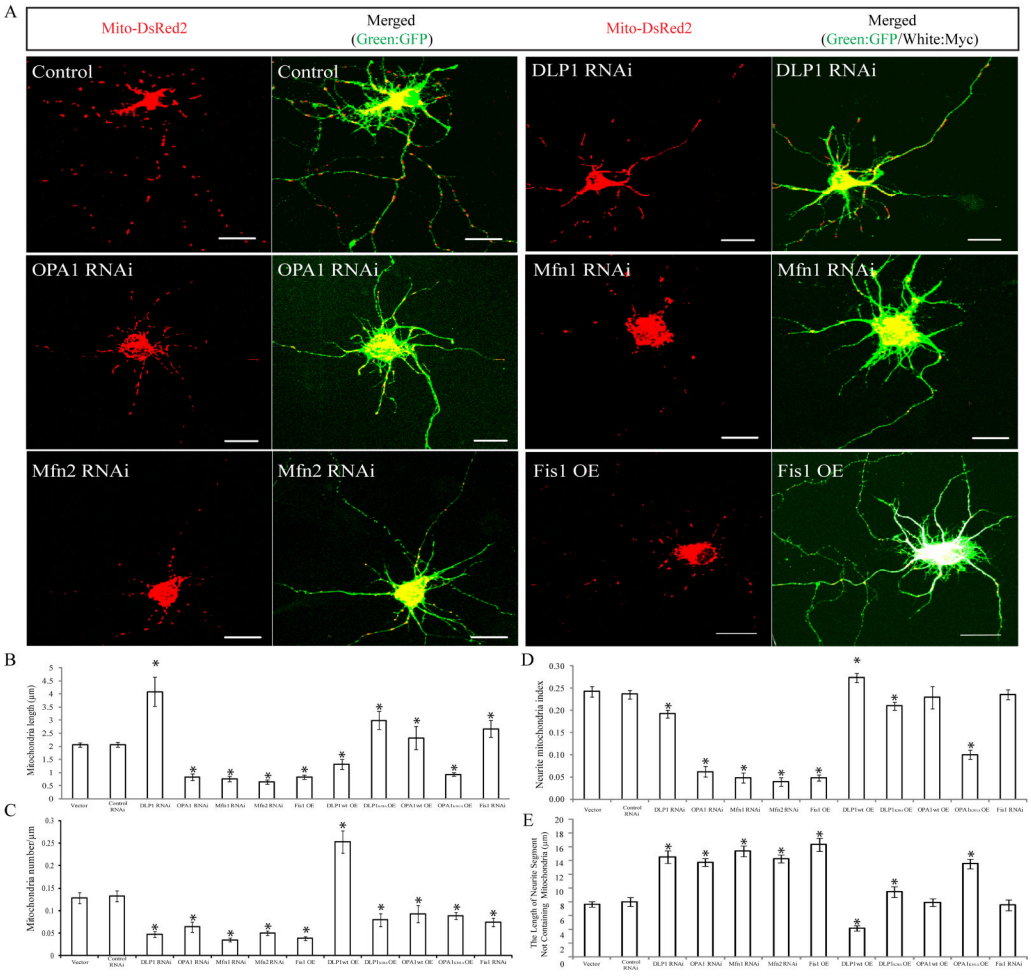

Figure 5.

Modulations of mitochondrial fission/fusion proteins, mimicking changes in AD, cause similar abnormalities in differentiated primary neuronal cells. (A) shows representative pictures of mitochondria in primary rat E18 hippocampal neurons (DIV 7-12) transiently transfected with GFP-tagged miR RNAi expression vector targeting DLP1, OPA1, Mfn1, or Mfn2 (DLP1, OPA1, Mfn1 or Mfn2 RNAi) or a myc-tagged Fis1 expression vector (Fis1 OE) and mito-DsRed2 (Red) to label mitochondria. For myc-tagged Fis1 overexpression, a GFP expressing vector was also co-transfected to show neurites and soma. Positively transfected cells were identified by GFP fluorescence (green) or Myc immunostaining (white). (B-E) are quantification of mitochondria length (B), number (C), neurite mitochondria index (total mitochondrial length/neurite length) (D) and axial length of neurites devoid of mitochondria (E) in a segment of neuronal process 400 μm in length beginning from the cell body of neurons either overexpressing or knocking down mitochondria fission/fusion proteins (*$p < 0.05$, student-t-test). All scale bars: 20 μm. At least 20 cells were analyzed in each experiment, experiments were repeated three times.

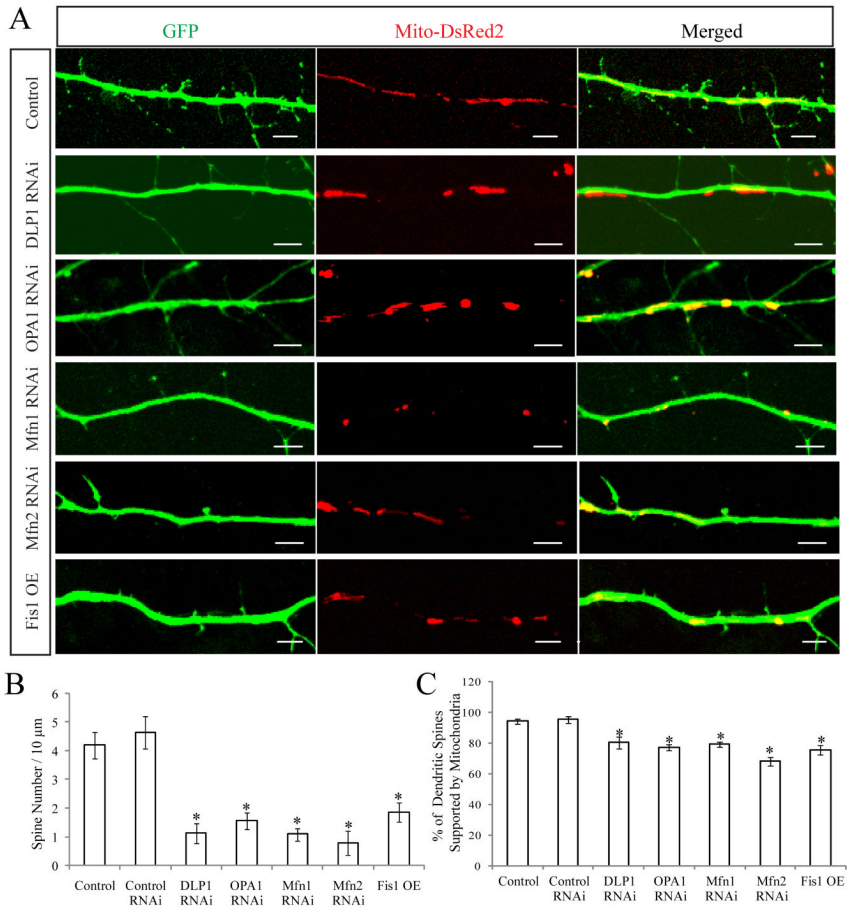

Figure 6.

Effect of mitochondria fission/fusion proteins on dendritic spines. Primary rat E18 primary hippocampal neurons were transfected at DIV 9 with indicated plasmids. For each neuron, dendritic segments 100-200 μm in length beginning 100 μm from the cell body were selected. Representative pictures of positively transfected neurons (A) were shown. (B) and (C) were quantification of spine number and the percentage of spines supported by mitochondria (*$p < 0.05$, student-t-test). All scale bars: 5 μm. At least 20 cells were analyzed in each experiment, experiments were repeated three times.

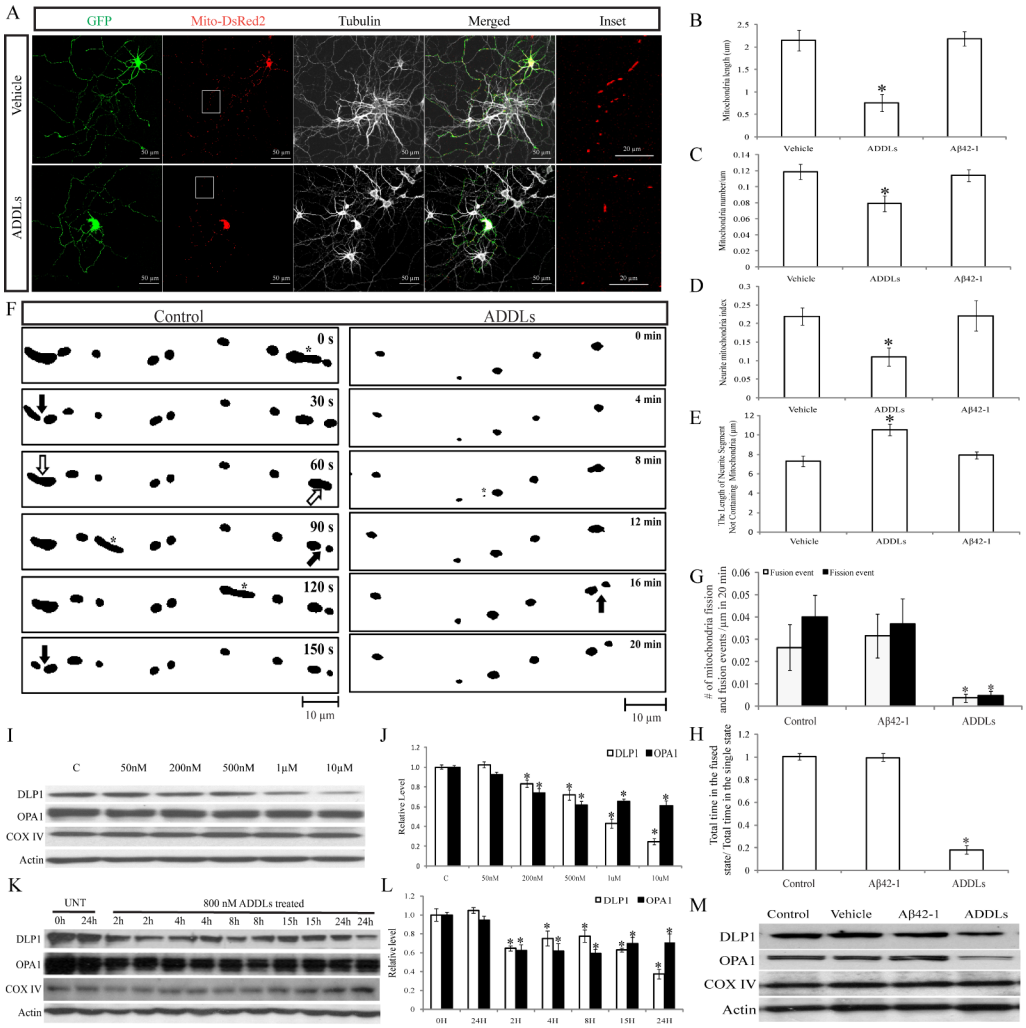

Figure 7.

Effects of ADDLs on mitochondrial morphology and distribution in primary neurons. Primary rat E18 hippocampal neurons (DIV9-12) transfected with GFP and mito-DsRed2 were treated with 800 nM ADDLs for 24 h. 24 hr treatment of $A\beta_{42-1}$, subject to the same procedure that produces ADDLs, was used as a control. Representative pictures (A) of positively transfected neurons were shown. Red: DsRed; green: GFP; white: Tubulin staining. (B-E) are quantification of mitochondria length (B), density (C), neurite mitochondrial index (D) and axial length of neurites devoid of mitochondria (E) in a segment of neuronal process 400 μm in length beginning from the cell body of neurons (*$p < 0.05$, student-t-test). At least 20 cells were analyzed in each experiment, experiments were repeated three times. (F) demosntrated the effect of ADDLs on mitochondria fission and fusion events. Rat E18 hippocampal neurons (DIV 9) were transfected with mito-DsRed2. 24 h after incubation with or without 800nM ADDLs at DIV 11, neurons were imaged in time-lapse (10s interval, 20 min). Representative thresholded time-lapse pictures (F) showed active mitochondria fission and fusion in the segment of axon around 100 μm in length beginning 300 μm from the cell body of control or ADDLs-treated neurons. Active mitochondria fission (filled arrow), fusion (hollowed arrow), and fast moving mitochondria (asterisks) are marked. Both fusion and fission were impaired

significantly by ADDLs (G), and mitochondria spent significantly less time in the post-fusion, “fused state” than in the post-fission, “single state” (H). At least 20 neurons were analyzed in three independent experiments (*$p < 0.05$, student t-test). (I-L) were immunoblot and quantitative analysis of DLP1 and OPA1 levels in neurons treated at indicated dosage of ADDLs for 24 hr (I and J) or at 800 nM for indicated period of time (K and L) revealed that ADDLs induced a dose- and time-dependent decrease in DLP1 and OPA1 levels (*$p < 0.05$, student-t-test). Unlike ADDLs, 10 μM $A\beta_{42\text{-}1}$ had no effect on the expression of DLP1 and OPA1 (M). Equal protein amounts (15 μg) were loaded. Actin immunoblot was used as an internal loading control.

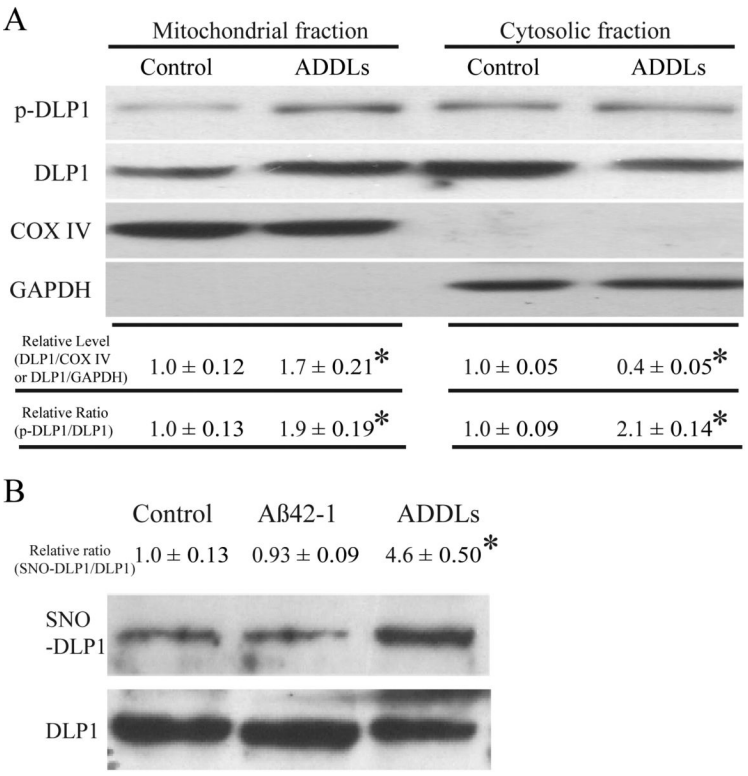

Figure 8.

Effects of ADDLs on sub-cellular localization and modification of DLP1 in primary rat E18 hippocampal neurons. Representative immunoblot and quantification analysis (A) showed that both relative mitochondrial DLP1 level (DLP1/COX IV) and the relative ratio of p-DLP1/DLP1 increased significantly in primary rat E18 hippocampal neurons (DIV 12) treated with 800 nM ADDLs for 24h. Unlike ADDLs, 10 μM $A\beta_{42\text{-}1}$ had no effect on either relative mitochondrial DLP1 level (DLP1/COX IV) or the relative ratio of p-DLP1/DLP1 (not shown). All samples were also immunoblotted with antibodies to detect mitochondrial (COX IV) and cytoplasmic (GAPDH) markers. The absence of GAPDH in the mitochondrial fraction confirms the purity of preparations from cell lysates. Representative immunoblot and quantification analysis (B) further revealed that SNO-DLP1 formation was also enhanced in primary rat E18 hippocampal neurons (DIV 12) treated with 800 nM ADDLs for 24h. As a control, 10 μM $A\beta_{42\text{-}1}$ did not affect SNO-DLP1 formation. All experiments were repeated three times (*$p < 0.05$, student-t-test).

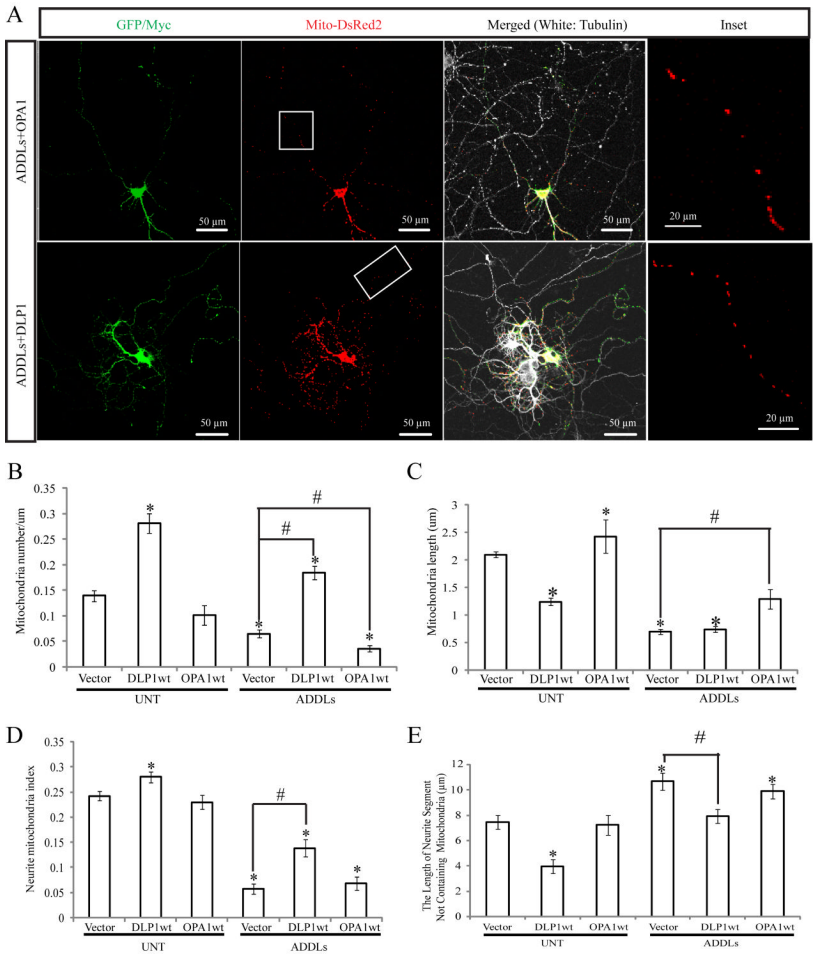

Figure 9.

Effects of DLP1 and OPA1 on ADDLs-induced mitochondrial dynamics changes. (A) showed representative pictures of neurons (DIV12) co-transfected with GFP, mito-DsRed2, and myc-tagged wild type DLP1 or wild type OPA1 after 24 h treatment with 800 nM ADDLs. Areas enclosed in white boxes were shown at larger magnification in Inset panel to allow better appreciation of changes in mitochondrial morphology and density. Red: DsRed; green: Myc; white: Tubulin staining. (B-E) were quantification of mitochondria number (B), length (C), neurite mitochondria index (D) and axial length of neurites not covered by mitochondria (E) in neurons with indicated treatment or manipulation (*$p < 0.05$, when compared to the nontransfected or empty-vector transfected normal control cells; #$p < 0.05$, when compared to control or empty-vector transfected cells with ADDLs treatment, student t-test). At least 20 neurons were analyzed in three independent experiments.

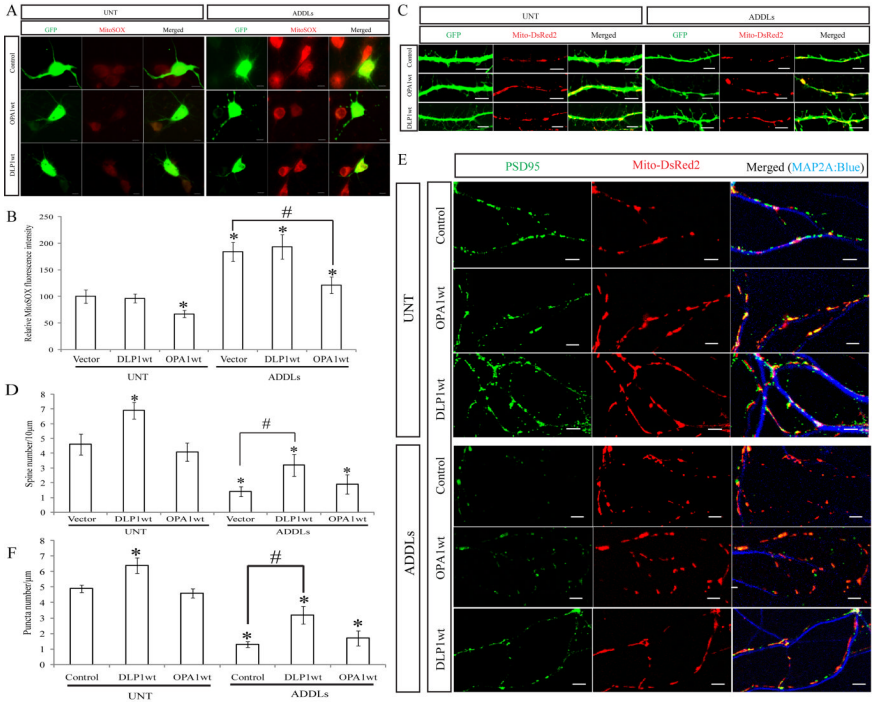

Figure 10.

Effects of DLP1 and OPA1 on ADDLs-induced changes in mitochondrial function and neuronal function. (A) and (B) were representative fluorescent pictures and quantification of mitochondria ROS in neurons (DIV12) transfected with GFP-tagged wild-type DLP1 or wild-type OPA1 with or without ADDLs treatment. Mitochondria ROS was labeled by mitoSOX; Positive transfected cells were selected by GFP signal. (C) and (D) were representative pictures and quantification of dendritic spine in neurons with or without ADDLs treatment. Neurons (DIV9) were co-transfected with GFP and myc-tagged wild type DLP1 or OPA1. Positive transfected cells were selected on the basis of GFP and myc staining. (E) and (F): To study the effect of Aβ on PSD-95, neurons (DIV9) were co-transfected with YFP tagged PSD-95 to label excitatory synapses, mito-DsRed2 to label mitochondria and myc tagged DLP1 or OPA1 constructs. (E) and (F) were representative pictures and quantification of PSD-95 puncta in neurons with or without ADDLs treatment and manipulation. Red: DsRed; green: YFP; blue: MAP2A. All scale bars: 5 μm. At least 20 neurons were analyzed in three independent experiments (*$p < 0.05$, when compared to the non-transfected or empty-vector transfected normal control cells; #$p < 0.05$, when compared to control or empty-vector transfected cells with ADDLs treatment, student t-test).